Title

Area/ Subarea

Name*

Department, University,

E-mail:

ICBR 2020

Abstract

Development of heterostructured semiconductor photocatalyst makes a significant advancement in catalytic technologies. Highly crystalline Bi_2S_3−ZnO nanosheets with hierarchical structure has been successfully synthesized by a facile sonochemical process and characterized by X−ray diffraction (XRD), High Resolution Scanning Electron Microscopy (HR−SEM), X-ray photoelectron spectroscopy (XPS), UV−Vis diffuse reflectance spectroscopy (DRS), Photoluminescence spectroscopy (PL) and Brunauer−Emmett−Teller (BET) surface area measurements. X-Ray powder diffraction (XRD) analysis reveals that the as synthesized product has orthorhombic phase of Bi_2S_3 and hexagonal wurtzite phase of ZnO. The XPS analysis shows the presence of Zn, O, Bi and S elements and their oxidation states. Bi_2S_3−ZnO has increased absorption in the UV as well as visible region. This heterostructured nano catalyst shows higher photocatalytic activity for the degradation of Acid Black1 (AB 1) under UV−A light than pure ZnO, Bi_2S_3 and commercial Degussa P25. The heterojunction in Bi_2S_3−ZnO photocataslyst led to the low recombination rates of photoinduced electron−hole pairs and enhanced photocatalytic activity. Bi_2S_3−ZnO is more advantageous in AB 1 degradation because of its reusability and higher efficiency at the neutral pH 7.

Introduction

❖ **Environmental Water pollution is one of the biggest problems that we face today. It is a global crisis that needs people in every country to work together, protecting our environment and improving before it's too late**

Use of non-toxic photocatalyst for removal of toxic dyes

Experimental Procedure

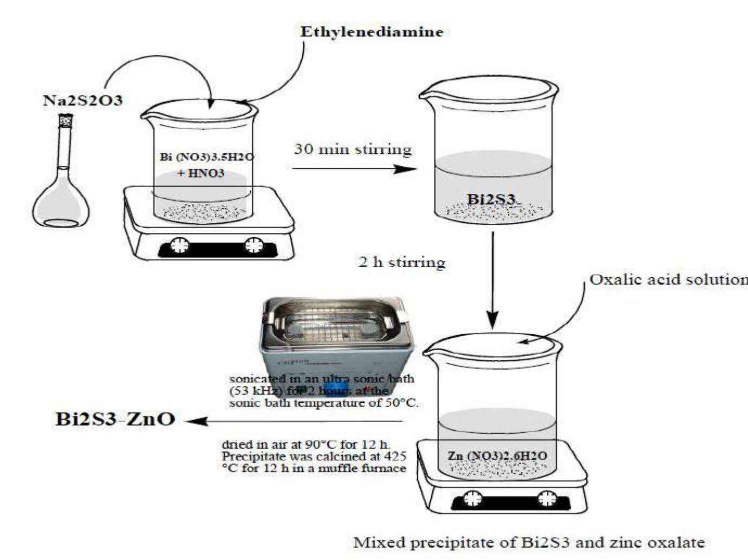

Results and Discussion

X-ray diffraction studies

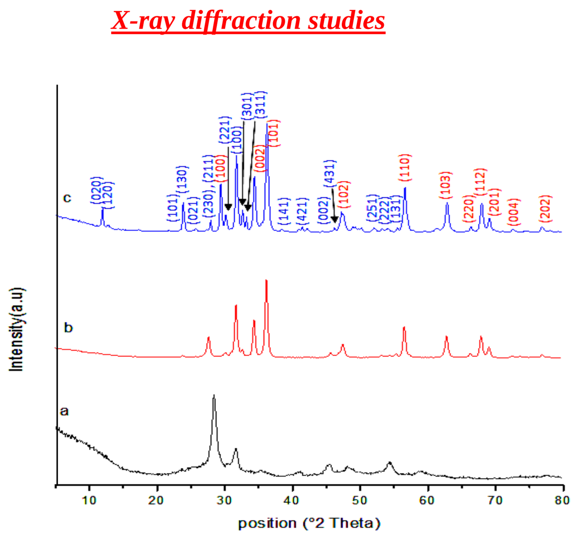

(a) Bi_2S_3 , (b) prepared ZnO and (c) Bi_2S_3-ZnO

➢ **All peaks of Bi_2S_3 and ZnO absolutely matched with Bi_2S_3−ZnO (Fig. c). XRD pattern of Bi_2S_3−ZnO reveals the presence of orthorhombic form of Bi_2S_3 in hexagonal wurtzite ZnO base material**

High-Resolution Scanning Electron Microscopy

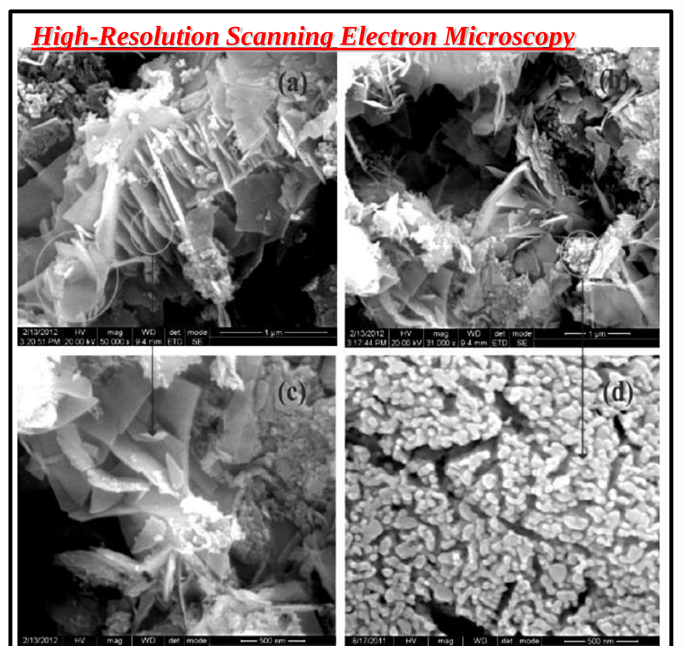

➢ **These images show that Bi_2S_3−ZnO is a mixture of nano sheets and nano particles The enlarged images confirm the heteroarchitectured form of the catalyst containing nanosheets and nanoparticles.**

➢ **The nanosheets have a breath of 34.2 nm with the length in the range of 240.9 to 656.8 nm (Fig. 2a).**

Field Emission Scanning Electron Microscopy

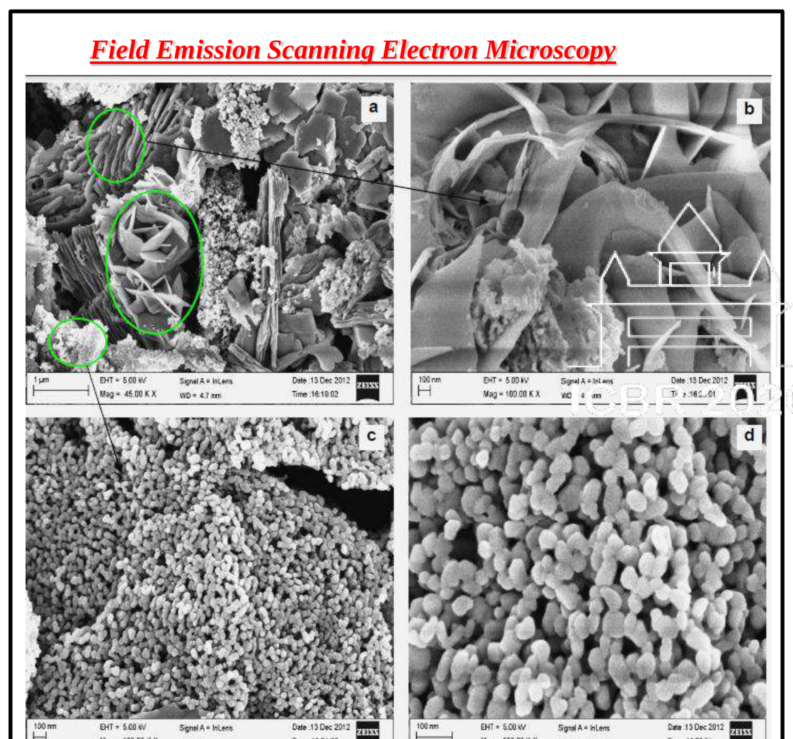

➢ **FESEM images shows a mixture of nanosheets and nano particles. The nanosheets attached with another nanosheet and form inter cross sectioned walls. The nanosheets were made up of Bi_2S_3 as confirmed by EDS analysis.**

➢**The nanoparticles were made up of ZnO. The nanoparticles have uniform structure and large number of cavities in the surface of Bi_2S_3-ZnO. These cavities favour the adsorption of dye molecules in the surfaces of the heteroarchitectured material.**

X-ray photoelectron spectroscopy

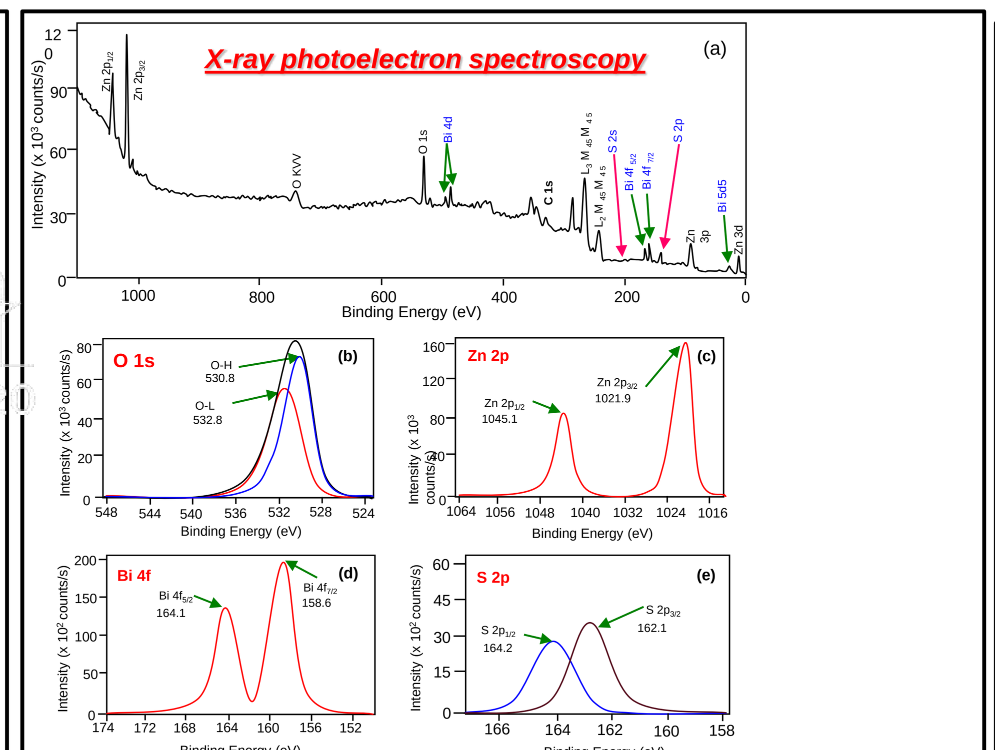

➢ **O1s profile is asymmetric and can be fitted to two symmetrical peaks α and β locating at 530.8 and 532.8 eV, respectively, indicating two different kinds of O species in the sample (Fig b). The peaks α and β should be associated with the lattice oxygen (O_L) of ZnO and chemisorbed oxygen (O_H) caused by the surface hydroxyl, respectively.**

➢ **Fig. c presents the XPS spectra of Zn 2p, and the peak positions of Zn $2p_{1/2}$ and Zn $2p_{3/2}$ locate at 1045.1 eV and 1021.9 eV. we can conclude that Zn is in the state of Zn^{2+}.**

The signals of Bi $4f_{7/2}$ and Bi $4f_{5/2}$ at 158.6 and 164.1 eV (Fig. d), reveal that Bismuth is in the state of Bi^{3+}.

➢ **Two signals of S $2p_{1/2}$ and S $2p_{3/2}$ at binding energies of 164.2 and 162.1eV indicate the presence of sulfide species S^{2-} (Fig. e).**

Diffuse Reflectance Spectra

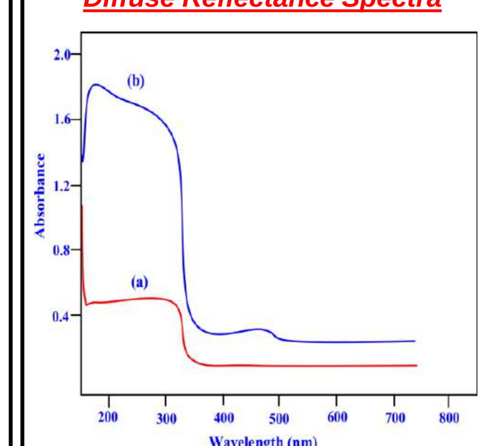

(a) prepared ZnO and (b) Bi_2S_3-ZnO

➢ **Bi_2S_3−ZnO shows many fold increased absorption in the ultraviolet region of 200-400 nm indicating more photocatalytic activity in UV.**

➢**There is a slight increase in absorbance in visible region.**

Photoluminescence Spectra

➢ **Catalysts show a near UV emission band at 416 nm and a blue–green band at 485 nm. This near UV emission corresponds to the exciton recombination related near−band edge emission of ZnO.**

➢ **Reduction of PL intensity at 416 nm for Bi_2S_3−ZnO when compared to prepared ZnO and Bi_2S_3 indicates the suppression of recombination of the photogenerated electron–hole pair by Bi_2S_3 loaded on ZnO. This leads to a higher photocatalytic activity.**

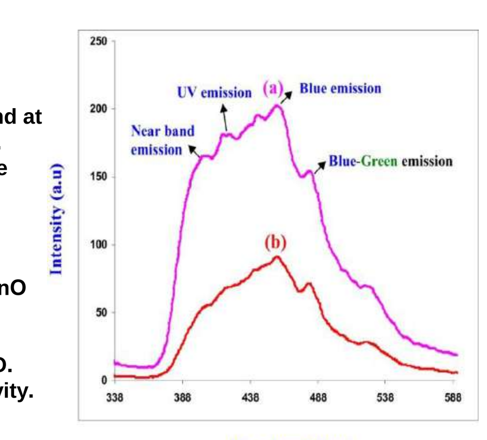

(a) prepared ZnO and (b) Bi_2S_3-ZnO

Photocatalytic activity

➢ **Dye is resistant to self photolysis. Under dark condition there is a decrease of dye concentration initially with Bi_2S_3−ZnO and this is due to adsorption of dye on the catalyst.**

➢ **Under UV−light irradiation, degradation of AB 1 occurred with all the catalysts. Almost complete degradation (96.0%) of dye was attained in 90 min with Bi_2S_3−ZnO and UV light. Percentages of degradation with ZnO, Bi_2S_3 and TiO_2−P25 were 76.1, 69.1 and 59 respectively for 90 min irradiation.**

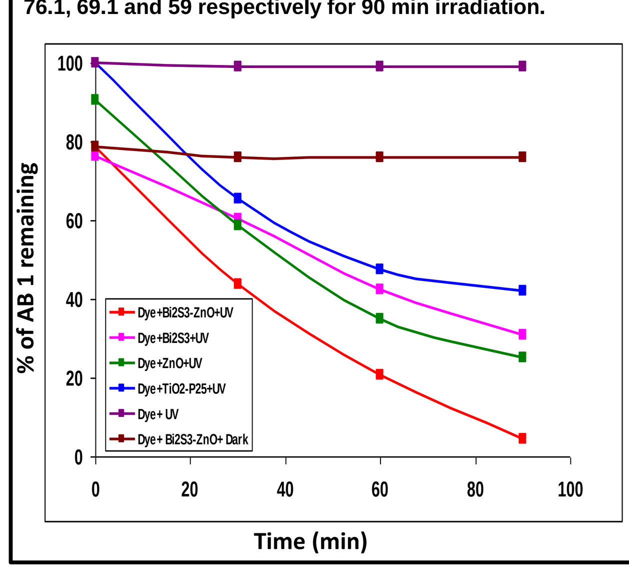

AB 1 dye with Bi_2S_3−ZnO under different irradiation times

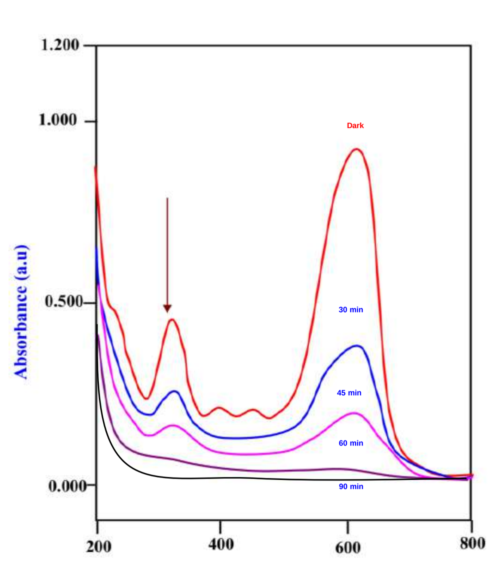

Effect of pH

➢ **After 90 min of irradiation the percentages of AB 1 degradation are 46, 73, 96, 63 and 32% at pH 3, 5, 7, 9 and 11, respectively. To find out the reason for the effect of pH on degradation efficiency, zero point charge (ZPC) of the catalyst was determined by potentiometric titration method.**

➢ **Zero point charge of Bi_2S_3-ZnO was found to be 7.3, which is less than ZPC of ZnO (9). When the pH is above ZPC, the surface charge density of the catalyst becomes negative. This decreases the adsorption of dye molecules, which exist anionic at pH above 7. Hence the degradation efficiency is low at pH 9 and 11.**

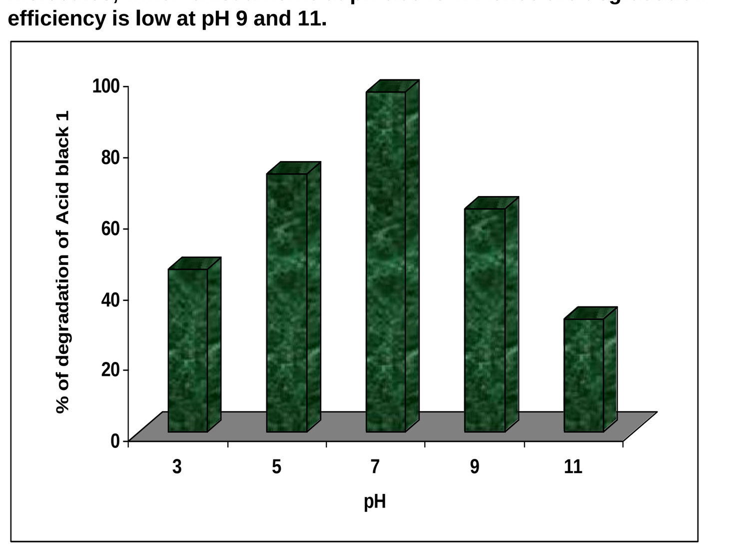

Reusability of the catalyst

➢ **Bi_2S_3−ZnO exhibits remarkable photostability as the AB 1 degradation percentages are 96.0%, 95%, 93%, 93% and 93% in the first, second, third, fourth and fifth runs respectively for 90 min. There is no significant change in the degradation efficiency of Bi_2S_3−ZnO after 3rd cycle.**

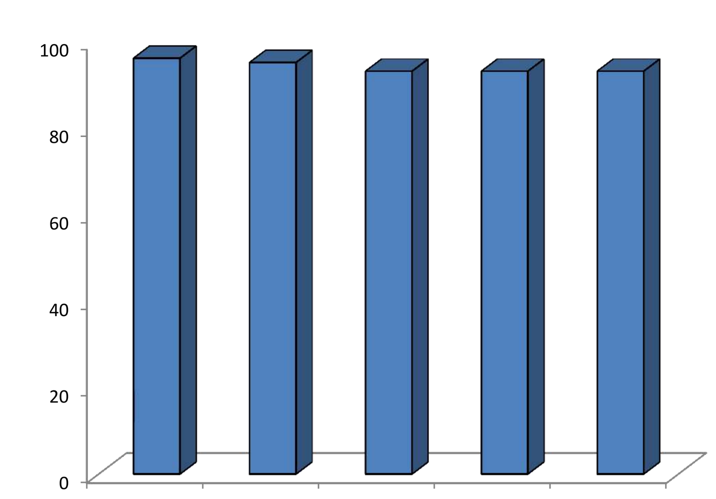

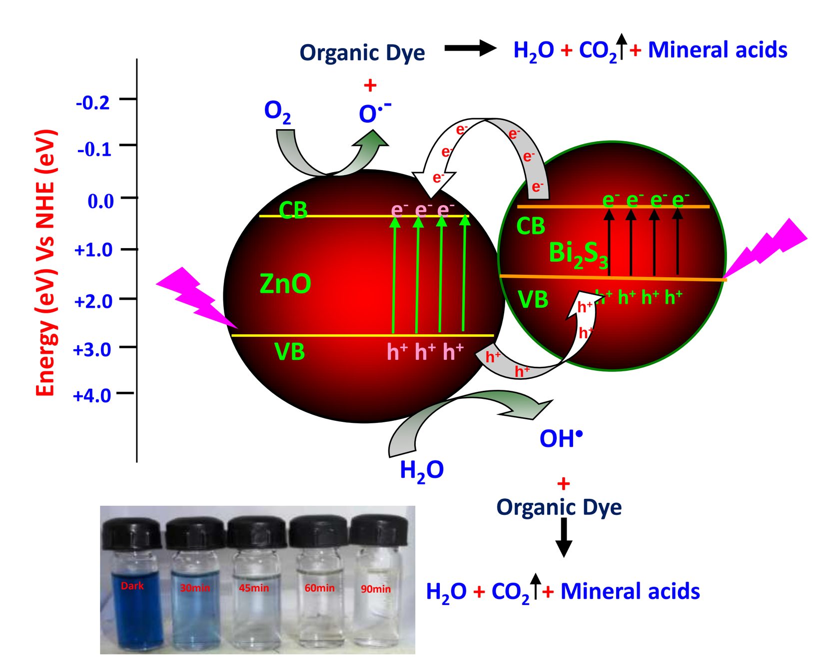

Conclusions

- **Bi_2S_3−ZnO semiconductor photocatalyst was synthesized by a simple and cost effective sonochemical method and characterized.**
- **XRD and XPS reveal the presence of Zn, O, Bi and S and their oxidation states in the catalyst.**
- **HR−SEM images show a mixed of nano sheets and nanoflower like hierarchical structure of Bi_2S_3−ZnO.**
- **Bi_2S_3−ZnO has many fold increase in UV absorption when compared to ZnO.**
- **The excellent photocatalytic activity stems from the different conduction band edge positions of Bi_2S_3 and ZnO, which promote electron transfer from Bi_2S_3 to ZnO and holes transfer from ZnO to Bi_2S_3 reducing electron-hole recombination.**
- **This heterojunction photocatalyst exhibits much enhanced photocatalytic activity in degradation of Acid Black 1 under UV light.**
- **Bi_2S_3−ZnO was found to be stable and reusable without appreciable loss of catalytic activity up to five runs. As this heterostructured catalyst is reusable with maximum efficiency at neutral pH 7 it will be very useful as industrial catalyst for effective treatment of dye effluents.**

References

1 A. McLaren, T. Valdes Solis, G. Li and S. C. Tsang, *J. Am. Chem. Soc.*, 2009, 131, 12540.

2 N. Kislov, J. Lahiri, H. Verma, D. Y. Goswami, E. Stefanakos and M. Batzill, *Langmuir*, 2009, 25, 3310.

3 M. D. Hernandez Alonso, F. Fresno, S. Sareza and J. M. Coronado, *Energy Environ. Sci.*, 2009, 2, 1231.

4 D. Yiamsawas, K. Boonpavanitchakul and W. Kangwansupamonkon, J. Microscopy. Soc.Thailand, 2009, 23, 75.

5J. F. Moudler, W. F. Stickle, P. E. Sobol and K. D. Bomben, Handbook of X-ray Photoelectron Spectroscopy Perkin-Elmer: Eden Prairie, MN, 1992.

6 C. D. Wagner, W. M. Riggs, L. E. Davis and J. F. Moulder, Handbook of X-ray Photoelectron Spectroscopy, Perkin Elmer: Eden Prairie, 1979, 81.

7 Y. Schuhl, H. Baussart, R. Delobel, M. Le Bras, J. Leroy, L. G. Gengembre and Rimblot, J. Chem. Soc. Faraday Trans., 1983, 79, 2055.

8 S. Subramanian, J. S. Noh and J. A. Schwarz, J. Catal., 1988, 114, 433.

9 R. Velmurugan, B. Krishnakumar, B. Subash and M. Swaminathan, Sol. Energy Mater. Sol. Cells, 2013, 108, 205-212.

10 D. K. Ma, M. L. Guan, S. S. Liu, Y. Q. Zhang, C. W. Zhang, Y. X. He and S. M. Huang, Dalton Trans., 2012, 41, 5581.